JOURNAL OF MAGNETIC RESONANCE **133,** 98–103 (1998)
ARTICLE NO. MN981435

Lithium Visibility in Rat Brain and Muscle *in Vivo* by ^{7}Li NMR Imaging

Richard A. Komoroski,*,†,‡,§ John M. Pearce,*,† and Joseph E. O. Newton§,¶

**Department of Radiology, †Department of Pathology, ‡Department of Biochemistry, §Department of Psychiatry, and ¶Department of Pediatrics, University of Arkansas for Medical Sciences, 4301 West Markham Street, Little Rock, Arkansas 72205*

Received July 15, 1997; revised December 11, 1997

The apparent concentration of lithium (Li) *in vivo* **was determined for several regions in the brain and muscle of rats by ^{7}Li NMR imaging at 4.7 T with inclusion of an external standard of known concentration and visibility. The average apparent concentrations were 10.1 mM for muscle, and 4.2–5.3 mM for various brain regions under the dosing conditions used. The results were compared to concentrations determined** *in vitro* **by high-resolution ^{7}Li NMR spectroscopy of extracts of brain and muscle tissue from the same rats. The comparison provided estimates of the ^{7}Li NMR visibility of the Li cation in each tissue region. Although there was considerable scatter of the calculated visibilities among the five rats studied, the results suggested essentially full visibility (96%) for Li in muscle, and somewhat reduced visibility (74–93%) in the various brain regions.** © 1998 Academic Press

Key Words: **visibility; bipolar disorder; manic-depressive; lithium analysis; quadrupolar.**

INTRODUCTION

Lithium (Li) is the treatment of choice for manic-depressive illness, also called bipolar disorder (*1*). Li treatment is usually monitored by determining the serum concentration of the ion. Although relatively easy and inexpensive to measure, the concentration in serum may be less than ideal for monitoring treatment. The magnitude of the pharmacologic effect of a drug depends on the concentration at the receptor sites in the target tissue, which may not be reflected in the serum concentration. Thus, the concentration of Li in the brain may be a better measure of Li therapy or toxic effects (*2, 3*). There is a need for a noninvasive, *in vivo* measure of Li concentration, particularly one that can be applied to humans. *In vivo* ^{7}Li NMR spectroscopy and imaging, which have been under development in several laboratories including our own, are potentially such methods (see Refs. *4* and *5* for reviews). Recent *in vivo* ^{7}Li NMR spectroscopic results for humans on Li therapy confirm that the correlation between serum and brain Li concentrations is weak or nonexistent (*6, 7*).

One advantage of NMR spectroscopy relative to other spectroscopies is that, when properly acquired, the NMR signal usually is proportional to the number of atoms of a given species. Sodium-23 and ^{39}K NMR studies on a wide variety of tissues have shown that the ion concentration determined from the NMR signal intensity is often substantially less than that determined by other analytical methods (*8, 9*). Lithium-7 has substantially different NMR properties from those of ^{23}Na or ^{39}K, which suggest that its visibility may, at most, be only slightly reduced from 100% in biological tissues, as has been observed in erythrocytes under certain conditions (*10–12*). The extent to which the ^{7}Li NMR signals from biological tissues exhibit reduced visibility *in vivo* has not been determined.

We have reported initial, primarily qualitative results on ^{7}Li NMR imaging, localized spectroscopy, and spin relaxation at 4.7 T *in vivo* on rat brain (*13*) under a variety of experimental conditions, without confirmation by chemical analysis. We recently reported apparent concentration ratios obtained by *in vivo* ^{7}Li NMR imaging of rat brain and muscle under standard conditions (*14*). However, for elucidation of the mechanism(s) of action of Li and for comparison to serum Li concentration and clinical status, a measure of actual brain concentration is desired. Here we report the use of an internal quantitation standard with ^{7}Li NMR imaging to obtain estimates of tissue Li concentration. These quantitative *in vivo* results are compared to results from *in vitro* analysis of brain and muscle extracts from the same rats by high-resolution ^{7}Li NMR spectroscopy (*15*). This provides estimates of the ^{7}Li NMR visibility of the Li cation in the various tissues *in vivo* in the rat, under one set of typical conditions. Such studies are necessary as a prelude to similar work on humans on clinical scanners.

RESULTS

Figure 1A shows a typical sagittal localizer ^{1}H NMR image of rat head with quantitation standard dimly apparent. In Fig. 1B is the corresponding ^{7}Li image, also with quantitation standard (100% visible, see Experimental) apparent, which is typical of that used to derive regional Li concentrations. In Table 1 are the apparent *in vivo* Li concentrations and visibilities, relative to high-resolution ^{7}Li NMR (*15*), for regions of brain and muscle in the five rats studied. The visibility is the ratio of the apparent *in vivo* concentration to the corresponding *in vitro* concentration. Thus, the *in vitro* concentrations can be recovered by dividing the apparent *in vivo* concentrations by the corresponding fractional visibilities.

1090-7807/98 $25.00

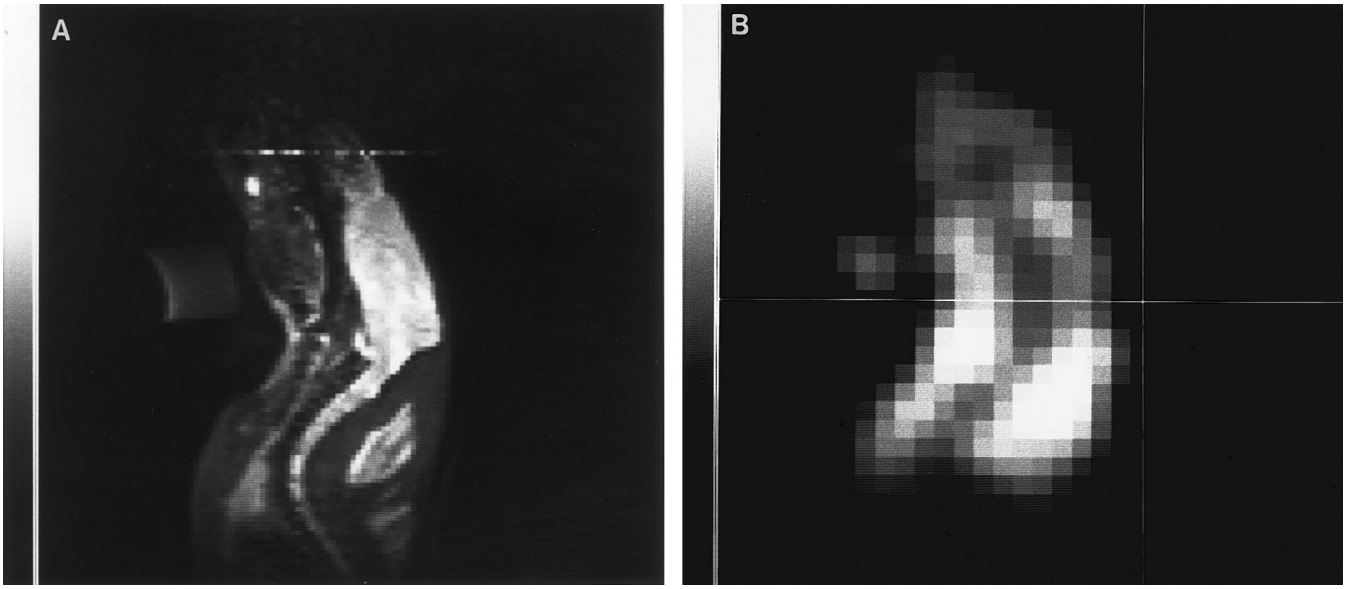

FIG. 1. (A) Sagittal ^{1}H NMR image of rat head (256 × 256 matrix; TE, 45 ms; TR, 3.6 s; 1 acquisition; 2-mm slice; FOV, 160 mm). (B) The corresponding *in vivo* ^{7}Li NMR image of rat head, typical of those used to obtain regional Li concentrations (64 × 64 matrix; TE, 3.8 ms; TR, 5.2 s; 108 acquisitions; 10-mm slice; FOV, 160 mm). The horizontal line at zero phase-encode gradient in the ^{1}H image is an artifact. The dim object under the head in both images is the Li standard. A magnetic susceptibility artifact is apparent on the left of the standard in the ^{1}H image. The standard appears curved because of nonlinear gradient performance under this ^{1}H imaging condition, which did not affect ^{7}Li imaging or quantitation.

In general, the visibilities are less than 100%. For a given region, particularly cerebellum and medulla, the visibility displays considerable scatter, as shown in Fig. 2. For muscle, the average visibility is only slightly reduced (96%), whereas for brain the average visibility varies from 74 to 93%, depending on region.

By *t*-test, there is no statistical difference ($p < 0.05$) between the *in vivo* results for muscle, cerebellum, or medulla, and the corresponding results *in vitro.* For the forebrain and midbrain regions, the *in vivo* concentrations are significantly reduced ($p < 0.018$) from the corresponding *in vitro* concentrations.

Using multivariate analysis of variance, there was no effect of region on the visibilities. However, the effect of region on the apparent *in vivo* concentration was highly significant [$F(4/16) = 42.1$, $p < 0.000001$]. *In vivo,* the results for muscle were significantly different from those of all other regions, and the results for forebrain were different from those of midbrain and medulla. Figure 3 shows a graphical comparison of the apparent *in vivo* concentrations for the various regions.

DISCUSSION

^{7}Li Visibility in Vivo

Interpretation of *in vivo* NMR spectra for spin-3/2 nuclei such as ^{23}Na, ^{39}K, and ^{7}Li can be complicated by several

TABLE 1
Apparent *in Vivo* Li Concentrations (mM) and ^{7}Li NMR Visibilities (%) Relative to *in Vitro* NMR

		Muscle		Forebrain		Midbrain		Cerebellum		Medulla	
Rat[a]	Delay[b]	Conc.	Visibility	Conc.	Visibility	Conc.	Visibility	Conc.	Visibility	Conc.	Visibility
1	10.5	10.2	94	4.9	73	4.4	83	4.7	105	4.7	117
2	11.1	11.3	80	6.8	88	6.3	82	5.9	88	5.7	104
3	11.7	9.6	106	5.4	82	4.5	73	4.4	102	4.2	
4	10.0	13.8	98	6.9	83	5.6	67	4.3	64	4.8	65
5	11.0	5.8	101	2.3	76	1.9	67	2.5	104	1.6	52
Avg.	10.9	10.1	96	5.3	80	4.5	74	4.3	93	4.2	84
s.d.	0.64	2.9	9.8	1.9	6.2	1.7	7.9	1.2	17.4	1.5	31

[a] Avg., average; s.d., standard deviation.
[b] Delay in hours between the last Li dose and beginning the *in vivo* ^{7}Li NMR scan.

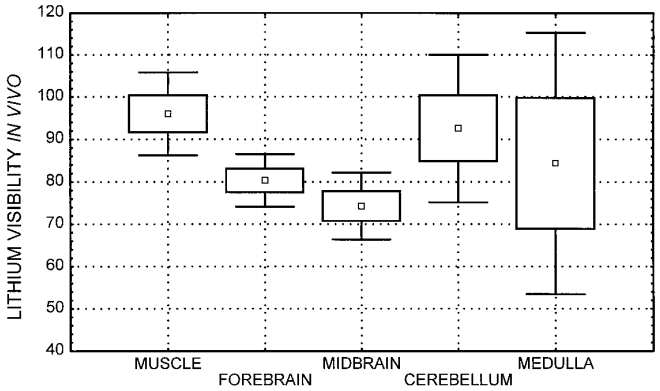

FIG. 2. Plot of mean *in vivo* ^{7}Li visibilities for various tissue regions relative to *in vitro* concentrations determined by high-resolution ^{7}Li NMR. The bars give standard deviations, and the rectangles standard errors of the mean.

factors. Sodium-23 and ^{39}K studies on a wide variety of tissues have shown that the ion concentration determined from the NMR signal intensity is often less than that determined by other analytical methods (*8, 9*). In the limit of rapid fluctuation of the electric field gradient tensor from rapid ionic and molecular motions, such as in aqueous solutions of alkali-metal salts, single exponential T_1 and T_2 relaxation times (and narrow Lorentzian NMR lines) are observed. When these fluctuations slow, as in a biological system, spin-3/2 nuclei such as ^{23}Na can exhibit an intrinsic biexponential relaxation, even when in a single molecular environment (*8, 9*). In the simplest case, theory predicts that T_1 consists of fast (20%) and slow (80%) relaxing components. For T_2 (and hence lineshape), the slowly relaxing or narrow component is 40% of the total intensity, and the rapidly relaxing or broad component is 60%.

In practice, depending on the details of the motional environment and the relaxation behaviors of the two components, 40–100% of the total signal will be observed under typical high-resolution conditions, where sampling of the FID is delayed by about 100–200 μs. Such intermediate visibilities can arise from partial detection of the fast-relaxing component, depending on the length of the data-sampling delay. Another possibility, pertinent to ionic species in biological systems, is the presence of a strongly bound, nonexchanging, and NMR-invisible fraction of ions. It is possible to observe less than 40% of the total signal if the narrow component is sufficiently broad. It is important to emphasize that these components are not separate ionic species, but can arise from all such nuclei in a single microscopic environment. A comprehensive theory based on a distribution of correlation times has been developed (*16, 17*).

The situation for spin-echo imaging is somewhat different in that here the echo at a specific TE (which is usually substantially longer than the high-resolution sampling delay mentioned earlier) is sampled. Depending on the magnitude of the specific T_2's characterizing the biexponential behavior relative to the TE, the visibility may be the same as or less than that observed in a comparable high-resolution spectrum. For spin-echo imaging, the measured visibility may be highly dependent on the particular pulse sequence parameters employed.

Lithium-7 has NMR properties and behavior substantially different from those of ^{23}Na or ^{39}K (*18*). Whereas ^{23}Na and ^{39}K relax totally and strongly by the quadrupolar mechanism, ^{7}Li is only weakly quadrupolar. This derives from the small quadrupole moment and Sternheimer antishielding factor of the Li^{+} cation (*18*). The Sternheimer antishielding factor is a measure of the effective electric field gradient at the nucleus from electron polarization caused by exposure of the cation to an external electric field gradient, such as with cation binding to a macromolecular site. The small value for Li relative to ^{23}Na or ^{39}K reflects Li's small size and simple electronic structure. Thus, ^{7}Li yields relatively long T_1's (2–15 s) and narrow resonance lines, relative to ^{23}Na ($T_1 \sim 10$–50 ms).

We previously found that ^{7}Li has substantial dipolar spin relaxation from interaction with ^{1}H in erythrocytes (*10*). At high concentrations (40 mM), ^{7}Li has 100% NMR visibility (*10–12*) for erythrocytes, which we found to be slightly reduced (84%) at 1 mM (*10*). No strongly bound fraction of Li or double-quantum behavior was seen (*10*). However, such a strongly bound, NMR-invisible fraction has been observed for Li in halotolerant bacteria (*19*).

The present results suggest essentially full visibility for ^{7}Li in muscle, and somewhat reduced visibility in brain under the single set of conditions used here. These conclusions are somewhat clouded by the considerable scatter in the visibility determinations, which probably arises from the necessarily low signal-to-noise (*S/N*) ratio of the ^{7}Li NMR image. In particular, the results for cerebellum and medulla are highly scattered, to the extent that there is no statistical difference between the *in vivo* and corresponding *in vitro* Li concentrations for these regions. For forebrain and midbrain, we can at this point report a reduced *in vivo* visibility with statistical confidence. The problem associated with low *S/N* ratio in the ^{7}Li images can be

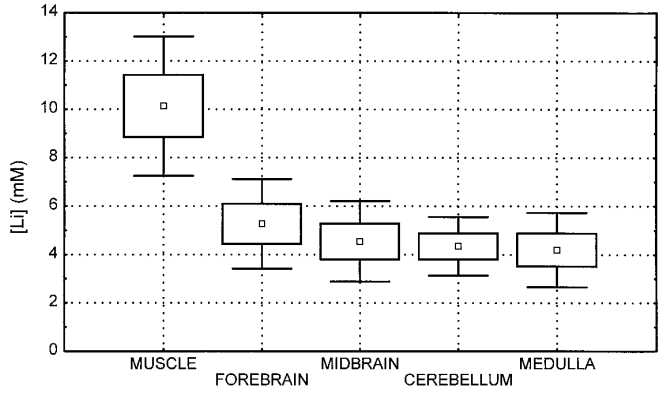

FIG. 3. Plot of mean apparent Li concentrations for rat muscle, forebrain, midbrain, cerebellum, and medulla, determined by *in vivo* ^{7}Li NMR imaging relative to a known standard. The bars give standard deviations, and the rectangles standard errors of the mean.

addressed by a visibility determination using localized spectroscopy, for which a larger voxel size will yield a larger *S/N* ratio, or other improvements in S/N ratio.

Our assumptions concerning T_1 and T_2 *in vivo* also require confirmation. If the *in vivo* T_1 is substantially longer (or the *in vivo* T_2 substantially shorter) than the preliminary value (*13*) used in our calculation, then the apparent Li concentration *in vivo* would be reduced. With our TR of 5.2 s, T_1 (typically about 3.5–4.6 s *in vivo*) affects the measured intensities. At our relatively short TE of 3.8 ms (for spin-echo NMR imaging), the influence of T_2 variations for any slowly relaxing component should be minimal. Variations in T_1 or T_2 among tissue regions, although not likely, could result in relative differences in reduced visibility among regions.

Sources of error associated with the *in vitro* determinations (*15*) or with partial volume effects in the *in vivo* image should be small relative to the low *S/N* problem discussed earlier.

It is legitimate to ask how relevant the present work is to the situation of ultimate interest—the state of Li *in vivo* in human brain as probed by ^{7}Li NMR on a clinical scanner at 1.5 T. Some differences are expected when employing an animal model because of the differing size, morphology, and neurochemistry of the brain. However, the similarity of spin relaxation times and other parameters for a particular NMR nucleus, including ^{7}Li, in similar tissues in different species suggests that reduced visibility will also be observed in human brain (*5*). The phenomenon of reduced visibility for spin-3/2 nuclei due to biexponential relaxation is not field dependent (*8*), and hence would be expected to occur in the same tissue at lower magnetic field also. Additional reduction of signal, arising from the particular choice of TE within the normal ranges for spin-echo imaging or localized spectroscopy on a clinical scanner, may also be observed. Thus, the ^{7}Li visibility measured on a clinical scanner may vary substantially from that determined here.

Li Distribution

Previous results on Li distribution in animal brain have been conflicting (*13*, *14*, and references therein). Although most studies concluded that the distribution of Li in brain is uneven, some reported relatively small variations of 20–30%, while others found large differences among different regions. Most studies agreed that muscle contains substantially more Li than brain, and that cerebellum and brain stem contain less Li than other brain regions. Our initial *in vivo* work found the ^{7}Li signal intensity in muscle to be about twice that overall in brain, with the level in cerebellum about 30% lower than that in the forebrain (*13*).

The present results are in agreement with our previous work (*13*). With the dosing protocol used here, we find the apparent Li concentration in muscle to be typically about 10 mM, twice the 4.2–5.3 mM found on average in the various brain regions. Forebrain had somewhat higher average apparent concentration (5.3 mM) than the other brain areas (4.2–4.5 mM).

Some individual variation in response to a constant Li dosage is expected. However, the tissue levels for one rat (#5, Table 1) fall about two standard deviations below the corresponding regional averages. A possible explanation for this relates to the ambiguity inherent in the ip method of Li administration. A single, ineffective dose in our three-dose protocol, particularly if it were the last dose, could result in substantially reduced tissue concentrations of Li. However, because we have no evidence to support this possibility, we attribute the deviation to abnormally efficient Li elimination in this particular animal.

CONCLUSIONS

The apparent concentration of Li *in vivo* was determined for several regions in the brain and muscle of rats by ^{7}Li NMR imaging at 4.7 T with inclusion of an external standard of known concentration and visibility. The average apparent concentrations were 10.1 mM for muscle, and 4.2–5.3 mM for various brain regions under the dosing conditions used. The results suggested essentially full visibility (96%) for Li in muscle, and somewhat reduced visibility (74–93%) in the various brain regions. The low *S/N* ratio of the visibility determinations and the considerable scatter in repeat measurements on different rats preclude a definitive statement on the extent of reduced visibility of ^{7}Li *in vivo*. Further work using localized spectroscopy for higher *S/N* ratio and more accurate, localized spin relaxation parameters is required.

EXPERIMENTAL

In Vivo Analysis

The procedures used here were approved by the Institutional Animal Care and Use Committee. Five male Sprague-Dawley rats weighing 200–380 g were administered Li intraperitoneally (ip) in a multiple-dose protocol consisting of two doses (morning and evening) of 5 meq/kg of aqueous LiCl on the first day, and 5 meq/kg on the morning of the next day. Anesthetization for ^{7}Li NMR imaging took place at 6–8 h after the last Li dose using 15 mg/kg xylazine followed by 80 mg/kg ketamine administered intramuscularly. Within 2 h, 1.5% isoflurane gas with oxygen was administered to prolong anesthetization. The magnet bore temperature was maintained at ambient with sufficient warm air flow.

Images were acquired at 10–12 h after the last Li dose (Table 1). Lithium-7 NMR images were acquired at 77.8 MHz on a General Electric Omega CSI-4.7 T system with a Sun Microsystems 3/160 computer and Acustar actively shielded gradients (0.2 T/m, bore diameter 155 mm). For localization, ^{1}H images were acquired at 200.1 MHz using conditions previously determined as optimum for brain visualization (*20*). Images for both nuclei were acquired using the two-coil assembly designed for these studies and described previously

(*13*). The size and B_1 field homogeneity of these coils were adequate for the present studies (*13*). Conventional spin-echo images were acquired with phase encoding along **z** (or **y**) and frequency encoding along **y** (or **z**). Since the ^{7}Li signal is much weaker than the ^{1}H signal, the ^{7}Li images were recorded at lower resolution and larger slice thickness. The raw ^{1}H data was double Fourier transformed after appropriate apodizations. The ^{7}Li data was handled similarly except that only one zero-filling was used in each dimension to yield a 64 × 64 matrix. The parameters for ^{1}H imaging were as follows: 256 × 256 matrix; echo time (TE), 45 ms; pulse delay (TR), 3.6 s; acquisitions, 1; slice thickness, 2 mm; field of view (FOV), 160 mm; in-plane resolution, 0.6 mm. For ^{7}Li imaging the parameters were 32 × 32 matrix; TE, 3.8 ms; TR, 5.2 s; acquisitions, 108; slice thickness, 10 mm; FOV, 160 mm; in-plane resolution, 5 mm; data accumulation time, 5 h.

A quantitation reference was prepared with relaxation parameters similar to those expected for ^{7}Li *in vivo,* permitting better optimization of acquisition parameters for the *in vivo* image than a LiCl solution. Melted agarose solution (2.6 mL of 4.0 mM LiCl, 2.5% w/w agarose powder and 0.35% $CuSO_4 \cdot 5H_2O$ in deionized water) was poured into a 4.5-mL polystyrene cuvette, and allowed to gel overnight at room temperature. The open end of the cuvette was trimmed to yield a 10 × 10 × 23 mm^3 volume and sealed with Teflon tape and Parafilm. During imaging, this reference was affixed above the throat of the supine rat with the longer axis horizontal, centered at midline and perpendicular to the coil/bore axis. The measured relaxation parameters of the standard were a T_1 of 3.1 s and a T_2 of 324 ms. To measure the ^{7}Li visibility of the reference, a one-pulse spectrum under quantitative conditions (90° RF pulse, 16 s TR) was obtained for the reference (vs a LiCl solution) centered in a 30-mL bottle containing an aqueous solution of LiCl (0.48 mM) and shift reagent (Na_3H_2TmDOTP · NaCl, 0.48 mM). The TmDOTP^{5-} is an NMR shift reagent, developed for separate observation of intracellular and extracellular cations *in vivo* (*21*), which is well suited for the present purpose. Using identical conditions, a spectrum was then obtained with the quantitation reference replaced by a cuvette containing 2.3 mL of aqueous 4.00 mM LiCl and 1% w/w $CuSO_4 \cdot 5H_2O$. The visibility so measured was 101%, which we take as full visibility (100%).

Regions of interest were located in the ^{1}H image. Raw image intensities were obtained at the corresponding coordinates in the ^{7}Li image. Limitations in ^{7}Li image resolution necessitated the selection of a single voxel to represent each region. A single voxel centered within the quantitation standard was also chosen. All voxels chosen were totally within the tissue of interest. The slice of 10-mm thickness was totally within brain (about 14 mm wide) at the points of interest. Thus, errors from partial volume effects were minimized to the extent possible within our experimental limitations. Depending on region and animal, the *S/N* ratios in a single voxel ranged from 4 to 22. The Li concentration at a given voxel was calculated by multiplying the standard concentration by the ratio of the raw intensities for region and standard after extrapolation to TE = 0 and infinite TR using ^{7}Li relaxation parameters reported previously for rat head (*13*), and measured for the standard. It was assumed that the ^{7}Li T_1 and T_2 did not vary substantially among the various tissue regions *in vivo* in a single animal, or among different animals.

In Vitro Analysis

Each rat was sacrificed at the end of the *in vivo* run by immersion in liquid N_2 for 24 s and dissected immediately. The rat brain was removed essentially intact and dissected into four regions (*22*): (1) forebrain and cortex; (2) ''midbrain,'' consisting of the remainder of cortex, hypothalamus, midbrain, and hippocampus; (3) cerebellum; (4) medulla oblongata and pons. Where possible, 0.5–1.0 cm^3 of neck muscle, approximately at dorsal midline, was also excised. All dissected tissue samples were stored at −70°C.

The Li extraction procedure was a modification of that used by Schou (*23*). The details of the sample preparation and quantitation have been reported elsewhere (*15*). A 2.5-mm o.d. spherical insert containing a shifted reference solution (5.00 mM LiCl, 1 mM Na_3H_2TmDOTP · NaCl in 15% D_2O at pH 6.6) was used for *in vitro* NMR quantitation. High-resolution ^{7}Li NMR spectra were acquired at ambient temperature at 116.8 MHz under quantitative conditions on a General Electric GN-300 spectrometer using a 10-mm broadband probe, 90° tip angle of 14.6 μs, 75-s pulse delay (based on a ^{7}Li T_1 of 14.8 s determined by inversion recovery on two samples), and signal averaging times of 2–8 h. The Li visibility *in vivo* was determined by dividing the apparent *in vivo* concentration (mM) by the corresponding *in vitro* concentration [mM, determined from tissue wet weight (*15*)].

Data were analyzed using the Pearson product-moment correlation, multivariate analysis of variance, and *t*-test for dependent samples in Statistica (Statsoft, Inc., Tulsa, OK).

ACKNOWLEDGMENTS

We thank A. Stone of the McClellan VA Hospital for performing the AA analyses. This work was supported by PHS Grant MH50469 to R.A.K.

REFERENCES

1. L. H. Price and G. R. Heninger, Lithium in the treatment of mood disorders, *New Engl. J. Med.* **331,** 591–598 (1994).
2. R. A. Komoroski, Measurement of psychoactive drugs in the human brain in vivo by MR spectroscopy, *Am. J. Neuroradiol.* **14,** 1038–1042 (1993).
3. R. A. Komoroski, In vivo NMR of drugs, *Anal. Chem.* **66,** 1024A–1033A (1994).
4. T. Kato, S. Takahashi, and T. Inubushi, Brain lithium concentration measured with lithium-7 magnetic resonance spectroscopy: A review, *Lithium* **5,** 75–82 (1994).

5. S. Ramaprasad and R. A. Komoroski, NMR imaging and localized spectroscopy of lithium, *Lithium* **5,** 127–138 (1994).
6. G. S. Sachs, P. F. Renshaw, B. Lafer, A. L. Stoll, A. R. Guimaraes, J. F. Rosenbaum, and R. G. Gonzalez, Variability of brain lithium levels during maintenance treatment: A magnetic resonance spectroscopy study, *Biol. Psychiatry* **38,** 422–428 (1995).
7. U. Riedl, A. Barocka, H. Kolem, J. Demling, W. P. Kaschka, R. Schelp, M. Stemmler, and D. Ebert, Duration of lithium treatment and brain lithium concentration in patients with unipolar and schizoaffective disorder—a study with magnetic resonance spectroscopy, *Biol. Psychiatry* **41,** 844–850 (1997).
8. C. S. Springer, Jr., Measurement of metal cation compartmentalization in tissue by high-resolution metal cation NMR, *Ann. Rev. Biophys. Biophys. Chem.* **16,** 375–399 (1987).
9. S. K. Miller and G. A. Elgavish, Shift-reagent-aided ^{23}Na NMR spectroscopy in cellular, tissue, and whole-organ systems, *Biol. Magn. Reson.* **11,** 159–240 (1992).
10. R. P. Gullapalli, R. M. Hawk, and R. A. Komoroski, A ^{7}Li NMR study of visibility, spin relaxation, and transport in normal human erythrocytes, *Magn. Reson. Med.* **20,** 240–252 (1991).
11. J. W. Pettegrew, J. F. M. Post, K. Panchalingam, G. Withers, and D. E. Woessner, ^{7}Li study of normal human erythrocytes, *J. Magn. Reson.* **71,** 504–519 (1987).
12. Q. Rong, M. Espanol, D. Mota de Freitas, and C. F. G. C. Geraldes, ^{7}Li NMR relaxation study of Li^{+} binding in human erythrocytes, *Biochemistry* **32,** 13490–13498 (1993).
13. S. Ramaprasad, J. E. O. Newton, D. Cardwell, A. H. Fowler, and R. A. Komoroski, In vivo ^{7}Li NMR imaging and localized spectroscopy of rat brain, *Magn. Reson. Med.* **25,** 308–318 (1992).
14. R. A. Komoroski, J. M. Pearce, and J. E. O. Newton, In vivo distribution of lithium in rat brain and muscle by ^{7}Li NMR imaging, *Magn. Reson. Med.* **38,** 275–278 (1997).
15. R. A. Komoroski, J. M. Pearce, and J. E. O. Newton, Distribution of lithium in rat brain and muscle: A comparison of ^{7}Li NMR and atomic absorption spectrophotometry in vitro, *J. Magn. Reson. Anal.* **3,** 169–173 (1997).
16. W. D. Rooney and C. S. Springer, Jr., A comprehensive approach to the analysis and interpretation of the resonances of spins 3/2 from living systems, *NMR Biomed.* **4,** 209–226 (1991).
17. W. D. Rooney and C. S. Springer, Jr., The molecular environment of intracellular sodium: ^{23}Na NMR relaxation, *NMR Biomed.* **4,** 227–245 (1991).
18. J. W. Akitt, The alkali and alkaline earth metals, in ''Multinuclear NMR'' (J. Mason, Ed.), Chapter 7, pp. 189–220, Plenum, New York (1987).
19. M. Goldberg, M. Risk, and H. Gilboa, Lithium nuclear magnetic resonance measurements in halotolerant bacterium B_{a1}, *Biochim. Biophys. Acta* **763,** 35–40 (1983).
20. Y.-L. Ting and P. Bendel, Thin-section MR imaging of rat brain at 4.7 T, *J. Magn. Reson. Imaging* **2,** 393–399 (1992).
21. N. Bansal, M. J. Germann, I. Lazar, C. Malloy, and A. D. Sherry, In vivo Na-23 MR imaging and spectroscopy of rat brain during $TmDOTP^{5-}$ infusion, *J. Magn. Reson. Imaging* **2,** 385–391 (1992).
22. J. Glowinski and L. L. Iversen, Regional studies of catecholamines in the rat brain—I, *J. Neurochem.* **13,** 655–669 (1966).
23. M. Schou, Lithium studies. 3. Distribution between serum and tissues, *Acta Pharmacol. Toxicol.* **15,** 115–124 (1958).